Primary cultures of human tracheal epithelial cells may demonstrate the real pathogenic influence of influenza viral infection on the damage, viral replication and inflammatory cytokine production in the airways because human tracheal epithelial cells cultured using the method that we reported previously (Yamaya et al., 1992) retain the functions of the original tissue. In the present study, we infected primary cultures of human tracheal epithelial cells with four strains of influenza virus and measured the magnitude of viral replication, cell damage and cytokine production. We also examined the relationships and mechanisms among viral replication, cell damage and cytokine production in the infection with the pandemic influenza virus [A/Sendai-H/N0633/2009 (H1N1) pdm09].

2. Materials and methods

2.1. Human tracheal epithelial cell culture

The isolation and culture of the human tracheal surface epithelial cells were performed as described previously (Yamaya et al., 2010) in a mixture of Dulbecco's modified Eagle's medium (DMEM)-Ham's F-12 (DF-12) medium containing 2% Ultroser G (USG) serum substitute. The tracheas used for the cell cultures were obtained from 23 patients after death (age, 72 ± 11 yr; 10 female and 13 male). This study was approved by the Tohoku University Ethics Committee.

2.2. Culture of Madin Darby Canine Kidney cells

Madin Darby Canine Kidney (MDCK) cells were cultured in T_{25} flasks in Eagle's minimum essential medium (MEM) containing 10% fetal calf serum (Numazaki et al., 1987; Yamaya et al., 2010). The cells were then plated in 96-well plates and cultured.

2.3. Viral stocks

Stocks of influenza viruses were generated by infecting human tracheal epithelial cells with four strains of influenza virus as follows: the pandemic A/H1 2009 virus [A/H1N1 pdm 2009, A/Sendai-H/N0633/2009 (H1N1) pdm09] and three strains of the human influenza virus [A/H1N1 Sendai, A/Sendai-H/108/2009/(H1N1); A/H3N2 New York, A/H3N2/New York/55/2004; A/H3N2 Aichi, A/Aichi/2/68 (H3N2)] (Yamaya et al., 2010). The cells were cultured in 24-well plates in 0.9 ml of DF-12 medium and 100 μl of MEM containing virus for 1 h. The culture supernatants containing virus were then removed, and the cells were cultured in DF-12 medium containing 2% USG at 37 °C in 5% CO_2-95% air. To obtain the influenza virus solution, the supernatants were collected.

To prepare the A/H1N1 pdm 2009 virus and the A/H1N1 Sendai virus, which was isolated during the 2008–2009 season, nasal swabs were collected from patients and suspended in MEM medium (Numazaki et al., 1987). The A/H3N2 New York virus and the A/H3N2 Aichi virus, which were passaged 5–7 times in MDCK cells, were also used for the generation of viral stocks.

2.4. Detection and titration of viruses

The detection and titration of influenza viruses in the culture supernatant were performed using the endpoint method (Condit, 2006) by infecting replicate MDCK cells in plastic 96-well plates with 10-fold dilutions of virus-containing supernatants, as previously described (Yamaya et al., 2010). The presence of the typical cytopathic effects of the influenza virus was then examined. The $TCID_{50}$ (TCID, tissue culture infective dose) was calculated using previously described methods (Condit, 2006), and the viral titers in the supernatants were expressed as $TCID_{50}$ units/ml (Yamaya et al., 2010).

2.5. Viral infection of the cells

The infection of human tracheal epithelial cells with influenza was performed using previously described methods (Yamaya et al., 2010). A stock solution of influenza virus was added to the cells in 24-well plates (400 μl in each well, 1.0×10^3 $TCID_{50}$ units/ml, 0.8×10^{-3} $TCID_{50}$ units/cell of the multiplicity of infection). After a 1-h incubation period, the viral solution was removed, and the cells were cultured in 1 ml of fresh medium at 37 °C in 5% CO_2-95% air.

2.6. Collection of the supernatants

The supernatant (300 μl) was collected 1 day (24 h) and 3 days (72 h) after infection, and the same volume (300 μl) of fresh medium was added. The entire supernatant volume (1 ml) was collected 5 days (120 h) after infection. Furthermore, when the influenza virus titers 7 days (168 h) after infection were measured, the supernatant (300 μl) was collected 1 day (24 h), 3 days (72 h) and 5 days (120 h) after infection, and the same volume (300 μl) of fresh medium was added. The entire supernatant volume (1 ml) was collected 7 days (168 h) after infection.

2.7. Measurement of airway epithelial cell damage

To examine the tracheal epithelial cell damage after influenza infection, the number of floating cells in the supernatants, which were detached from the cell sheets adhered on the culture vessels of 24-well plates, and the number and viability of the adhered cells were measured by trypan blue exclusion. Lactate dehydrogenase (LDH) concentrations in the supernatants were also measured. These parameters demonstrate apoptosis and necrosis (Catalani et al., 2013; Cechetti et al., 2007; Yan et al., 2013).

2.8. Quantification of influenza virus RNA

Viral RNA in the cells was measured to confirm differences in the magnitude of viral replication among the species. A two-step real-time quantitative reverse transcription (RT)-PCR was performed using the TaqMan® Gene Expression Master Mix (Applied Biosystems, Bedford, CA, USA) as described previously (Yamaya et al., 2010). The primers and TaqMan probe for the viruses were designed as previously reported (Lorusso et al., 2010; Yamaya et al., 2010). The expression of viral RNA was normalized to the constitutive expression of β-actin mRNA (Suzuki et al., 2002).

2.9. NF-kappa B assay

The presence of p50 and p65 subunits in the nuclear extracts was assayed using a TransFactor Family Colorimetric Kit-NF-κB (BD Bioscience/CLONTECH) as previously described (Yamaya et al., 2011).

2.10. Measurement of cytokine production

We measured IL-6, TNF-α and IFN-γ levels in the supernatants. The measurement of IL-6 and INF-γ was performed using specific enzyme-linked immunosorbent assays (ELISA), and the measurement of TNF-α was performed using chemiluminescent enzyme immunoassay.

2.11. Statistical analysis

The results are expressed as the mean ± SEM. The statistical analysis was performed using a two-way repeated measures

analysis of variance (ANOVA). Subsequent post-hoc analyses were performed using Bonferroni's method. For all of the analyses, values of $p < 0.05$ were assumed to be significant. In the experiments using human tracheal epithelial cell cultures, n refers to the number of donors (tracheae) from which the cultured epithelial cells were obtained.

3. Results

3.1. Influenza virus release from airway epithelial cells

All four influenza virus strains that were tested, including the pandemic A/H1N1 2009 virus (A/H1N1 pdm 2009) and three strains of type A seasonal human influenza virus (A/H1N1 Sendai, A/H3N2 New York and A/H3N2 Aichi), were detected in the supernatants at 24 h, and the viral titers increased progressively between 24 h and 3 days after infection (Fig. 1A). The influenza virus titers of the four strains in the supernatants increased with time during the 3 days of observation ($p < 0.05$ in each case by ANOVA), and consistent viral titers were observed for 5 days after infection (Fig. 1A). Furthermore, consistent titers of the four strains of type A influenza virus were observed between day 5 and day 7. By contrast, the influenza viral titers of the four strains in the supernatants started to decline on day 7 after infection ($p < 0.05$). The influenza viral titers of the four strains 7 days after infection were as follows (mean ± SEM, $n = 5$): 5.6 ± 0.4 for the A/H1N1 pdm 2009 virus, 5.2 ± 0.4 for the A/H1N1 Sendai virus, 3.1 ± 0.3 for the A/H3N2 New York virus and 1.2 ± 0.3 for the A/H3N2 Aichi virus.

The viral titers of the A/H1N1 pdm 2009 virus and the A/H1N1 Sendai virus were higher than the titers of the A/H3N2 New York virus and the A/H3N2 Aichi virus (Fig. 1A and B). Furthermore, the titers of the A/H3N2 New York virus were higher than those of the A/H3N2 Aichi virus (Fig. 1A and B).

3.2. The number of detached cells after influenza viral infection

The number of detached cells in the supernatants 5 days after the sham infection with the DF-12 medium containing 2% USG was $0.8 \pm 0.1 \times 10^4$ (/well of 24-well plates, $n = 4$). The number of detached cells 5 days after the infection with four strains of virus was higher than the number of detached cells after the sham infection (Fig. 1C).

The number of detached cells after infection with the A/H1N1 pdm 2009 virus and the A/H1N1 Sendai virus was higher than the number after infection with the A/H3N2 New York virus and the A/H3N2 Aichi virus (Fig. 1C). Furthermore, the number of detached cells after infection with the A/H3N2 New York virus was higher than the number after infection with the A/H3N2 Aichi virus (Fig. 1C).

3.3. LDH release after influenza viral infection

The concentration of LDH in the supernatants 5 days after the sham infection was 34 ± 3 units/l ($n = 4$). The concentration of LDH 5 days after the infection with four strains of virus was higher than the concentration of LDH after the sham infection (Fig. 1D).

The concentration of LDH after the infection with the A/H1N1 pdm 2009 virus and the A/H1N1 Sendai virus were higher than the concentration of LDH after infection with the A/H3N2 New York virus and the A/H3N2 Aichi virus (Fig. 1D). The LDH levels after infection with the A/H3N2 New York virus were higher than the LDH levels after infection with the A/H3N2 Aichi virus (Fig. 1D).

3.4. Cytokine production after influenza viral infection

A significant amount of IL-6 in the supernatants was detected before viral infection (211 ± 13 pg/ml, $n = 4$) and 5 days after sham infection (Fig. 1E). The IL-6 levels increased after infection with the four strains of influenza virus (Fig. 1E). Maximum IL-6 levels were observed 5 days after infection with the four strains of influenza virus (data at 1 day, 3 days and 7 days not shown).

The IL-6 levels after infection with the A/H1N1 pdm 2009 virus and the A/H1N1 Sendai virus were higher than the IL-6 levels after infection with the A/H3N2 New York virus and the A/H3N2 Aichi virus (Fig. 1E). Furthermore, the IL-6 levels after infection with the A/H3N2 New York virus were higher than the levels after infection with the A/H3N2 Aichi virus (Fig. 1E).

In contrast, the concentration of TNF-α in the supernatants before infection was below the limits of detection (<0.55 pg/ml). TNF-α levels increased after infection with the four strains of virus, and significant amounts of TNF-α were detected after viral infection. TNF-α levels increased after infection with the four strains of virus as follows: 20 ± 2 pg/ml ($n = 4$) in the A/H1N1 pdm 2009 virus, 23 ± 2 pg/ml ($n = 4$) in the A/H1N1 Sendai virus, 11 ± 2 pg/ml ($n = 4$) in the A/H3N2 New York virus and 3 ± 1 pg/ml ($n = 4$) in the A/H3N2 Aichi virus. TNF-α levels after infection with the A/H1N1 pdm 2009 virus and the A/H1N1 Sendai virus were higher than the levels after infection with the A/H3N2 New York virus and the A/H3N2 Aichi virus ($p < 0.05$). The TNF-α levels after infection with the A/H3N2 New York virus were higher than the levels after infection with the A/H3N2 Aichi virus ($p < 0.05$).

The concentration of IFN-ϒ, measured using ELISA method, was below the limits of detection (<0.69 pg/ml).

3.5. NF-κB activation after influenza viral infection

A significant amount of the NF-κB p50 and p65 subunits was detected in the nuclear extracts from the vehicle-treated cells without influenza viral infection (Fig. 2). Infection with four strains of the influenza virus increased the amounts of the p50 and p65 subunits 5 days after infection (Fig. 2).

Significant differences in the amounts of NF-κB p50 in nuclear extracts were not observed among the cells infected with the four strains of influenza virus (Fig. 2A).

In contrast, the amounts of NF-κB p65 after infection with the A/H1N1 pdm 2009 virus and the A/H1N1 Sendai virus were higher than the amounts in the cells infected with the A/H3N2 New York virus and the A/H3N2 Aichi virus (Fig. 2B). Furthermore, the amounts of NF-κB p65 after infection with the A/H3N2 New York virus were higher than the amounts after infection with the A/H3N2 Aichi virus (Fig. 2B).

3.6. Effects of NF-kappa B inhibitor, anti-IL-6 antibody and caspase-3 inhibitor

We also studied the roles of NF-κB, IL-6 and caspase-3 on A/H1N1 pdm 2009 viral infection-induced cell damage and viral replication. The cells were treated with either an NF-κB inhibitor, caffeic acid phenethyl ester (CAPE, Calbiochem, La Jolla, CA, USA; 1 μM) (Natajaran et al., 1996), a monoclonal anti-IL-6 receptor antibody (R & D Systems Inc, MN, USA, 1.0 μg/ml) (Hsu et al., 2011), or a caspse-3 inhibitor, benzyloxycarbonyl-DEVD-fluoromethyl ketone (Z-DEVD-fmk) (Bio Vision, 1 μM) (Nicholson et al., 1995) from 30 min prior to viral infection until the measurement of the functions after infection.

The A/H1N1 pdm 2009 viral infection increased the number of detached cells in the supernatants (Fig. 3A and B), increased the number of dead cells in the attached cells and reduced the viability of the attached cells (Fig. 3C and D), although the viability changes

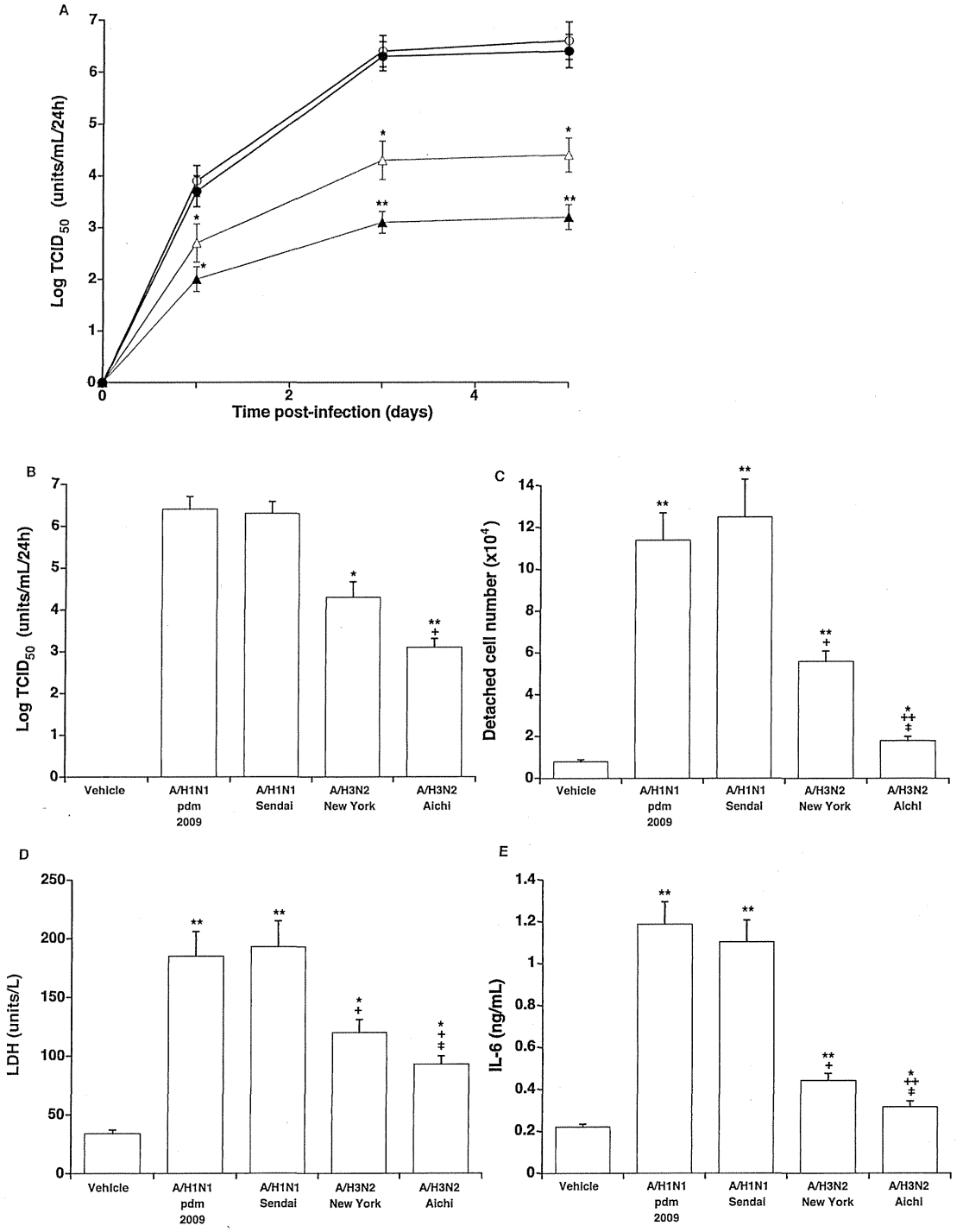

Fig. 1. (A) The time course of viral release into the supernatants of primary cultures of human tracheal epithelial cells obtained at different times after exposure to A/H1N1 pdm 2009 (open circles), A/H1N1 Sendai (closed circles), A/H3N2 New York (open triangles) and A/H3N2 Aichi (closed triangles) influenza viruses. Changes in the virus concentration in the supernatants are expressed as $TCID_{50}$ units/ml/24 h. The results are expressed as the mean ± SEM from four different tracheae. (B) Viral titers in the supernatants 5 days after exposure to the A/H1N1 pdm 2009, A/H1N1 Sendai, A/H3N2 New York and A/H3N2 Aichi viruses. Changes in the virus concentration in the supernatants are expressed as $TCID_{50}$ units/ml/24 h. The results are expresses as the mean ± SEM from four different tracheae. Significant differences from infection with the A/H1N1 pdm 2009 virus and the A/H1N1 Sendai virus are indicated by * $p < 0.05$ and ** $p < 0.01$. Significant differences from infection with the A/H3N2 New York virus are indicated by $^{+}$ $p < 0.05$. (C)–(E): The number of detached cells (C), concentration of LDH (D) and IL-6 (E) in the supernatants 5 days after exposure to the A/H1N1 pdm 2009, A/H1N1 Sendai, A/H3N2 New York and A/H3N2 Aichi viruses. The results are expressed as the mean ± SEM from four different tracheae. Significant differences from the sham infection (Vehicle) are indicated by * $p < 0.05$ and ** $p < 0.01$. Significant differences from infections with the A/H1N1 pdm 2009 virus and the A/H1N1 Sendai virus are indicated by $^{+}$ $p < 0.05$ and $^{++}$ $p < 0.01$. Significant differences from infection with the A/H3N2 New York virus are indicated by ‡ $p < 0.05$.

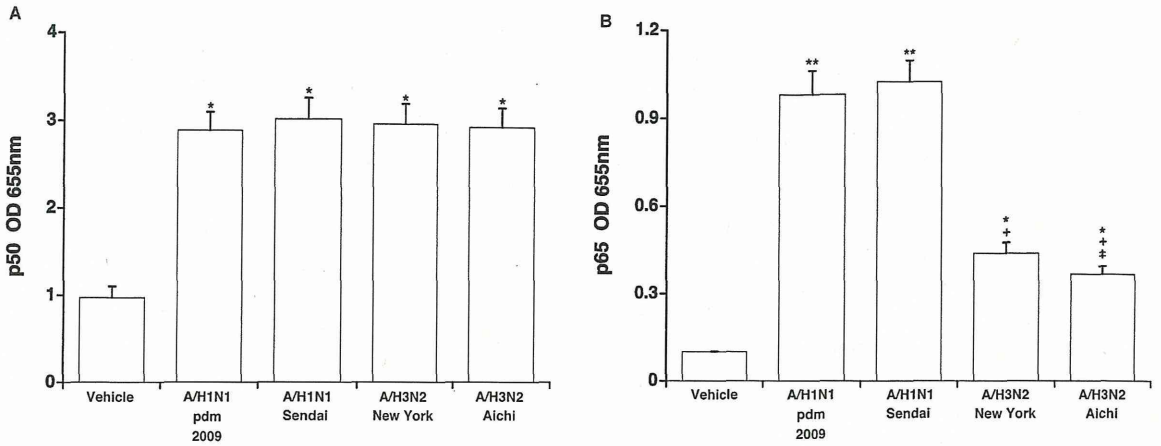

Fig. 2. (A) and (B) Amount of p50 (A) and p65 (B) in the nuclear extracts of cells 5 days after exposure to the A/H1N1 pdm 2009, A/H1N1 Sendai, A/H3N2 New York and A/H3N2 Aichi viruses. The results are expressed as the optical density (OD) and are the means ± SEM from four tracheae. Significant differences from the sham infection (Vehicle) are indicated by * $p < 0.05$ and ** $p < 0.01$. Significant differences from infections with the A/H1N1 pdm 2009 virus and the A/H1N1 Sendai virus are indicated by $^{+}$ $p < 0.05$. Significant differences from infection with the A/H3N2 New York virus are indicated by ‡ $p < 0.05$.

were small. The virus infection also increased the LDH concentration in the supernatants (Fig. 3E). Treatment with CAPE reduced the number of detached cells (Fig. 3A and B), reduced the number of dead cells, increased the viability of the cells and reduced the concentration of LDH (Fig. 3C–E) after the viral infection.

Treatment with CAPE also slightly, but significantly, reduced the A/H1N1 pdm 2009 viral titers in the supernatants and the viral RNA in the cells compared with the viral titers and viral RNA in the vehicle-treated cells (0.005% ethanol) (Fig. 3F and G).

Treatment with a monoclonal anti-IL-6 receptor antibody reduced the number of detached cells (Fig. 3A and B), reduced the number of dead cells, increased the viability of the cells and reduced the concentration of LDH (Fig. 3C–E) after the viral infection. Similarly, a monoclonal anti-IL-6 receptor antibody reduced the A/H1N1 pdm 2009 viral titers and viral RNA compared with the viral titers and viral RNA in the vehicle-treated cells (Fig. 3F and G).

Treatment with Z-DEVD-fmk (1 μM) reduced the number of detached cells and viral titers in the supernatants, but did not affect the concentration of LDH (Table 1) after the viral infection. In contrast, treatment with 10 μM Z-DEVD-fmk (Wen et al., 2010) induced cell damage in the absence of viral infection.

4. Discussion

We demonstrated that infection with four strains of type A influenza virus increased the detached cell number and the LDH levels in the supernatants of primary cultures of human tracheal epithelial cells. The detached cell number and the LDH levels were related to the viral titers, IL-6 levels and NF-κB p65 activation. Treatment with an NF-κB inhibitor (CAPE) (Natajaran et al., 1996) and an anti-IL-6 antibody reduced the detached cell number, dead cell number (in the attached cell sheets), LDH levels, viral titers and viral RNA, and improved the viability of the adhered cell sheets after the pandemic influenza virus infection. These findings suggest that influenza viral infection-induced cell damage may be partly associated with the magnitude of viral replication and subsequent NF-κB-p65-mediated IL-6 production.

IL-6 is associated with the pathogenesis of emphysematous changes through lung apoptosis in mice (Ruwanpura et al., 2011). IL-6 and TNF-α are also associated with cell death and the activation of caspases in swine macrophages after pandemic A/H1N1 viral infection (Gao et al., 2012). In contrast, in the present study, the IL-6 levels (>1 ng/ml) were much higher than the TNF-α levels (<0.03 ng/ml). A monoclonal anti-IL-6 receptor antibody and a NF-κB inhibitor (CAPE) partly reduced the detached cell number, dead cell number (of the adhered cell sheets) and LDH levels, and improved the viability of the adhered cell sheets. The concentration of IFN-γ was below the limits of detection. These findings suggest that IL-6 might be partly associated with cell damage after an influenza viral infection. However, the roles of other factors and mediators that are produced influenza viral infection, including IL-1β, IL-8 (Yamaya et al., 2010) and reactive oxygen species (Kim et al., 2013), remains to be examined; however, conflicting effects of IL-1β on apoptosis (Coulter et al., 2002; Lu et al., 2014) and the anti-apoptotic effects of IL-8 (Gyanchandani et al., 2013) have been demonstrated.

The NS1 protein coded in the non-structural (NS) gene-segment acts to inhibit the host interferon response, leads to the high expression of TNF-α and enhances the virulence of the H5N1 virus (Cheung et al., 2002; Garcia-Sastre et al., 1998). By contrast, the NS1 protein of the A/H1N1 2009 virus differs from the protein of H5N1 with high virulence (Shelton et al., 2012). These characteristics are consistent with a report stating that the virulence of the pandemic influenza virus was not extremely high compared with the virulence of seasonal influenza viruses (Presanis et al., 2009) and that the virulence may be associated with similar cytotoxic effects of the A/H1N1 pdm 2009 and A/H1N1 Sendai viruses, as observed in the present study.

The reasons why an anti-IL-6 receptor antibody and CAPE reduced viral release and viral RNA replication are uncertain. However, IL-6 activates caspases (Cai et al., 2012) that enhance the release of viral ribonucleoprotein complexes from the nucleus (Wurzer et al., 2003). A caspase-3 inhibitor Z-DEVD-fmk reduced the A/H1N1 pdm 2009 viral titers in the supernatants in the present study. Acetylsalicylic acid also blocks influenza viral propagation via its NF-κB-inhibiting activity (Mazur et al., 2007). The IL-6

Table 1
Effects of a caspase-3 inhibitor on the viral titers and the cell damage after influenza virus infection.

	A/H1N1 pdm 2009 + vehicle	A/H1N1 pdm 2009 + Z-DEVD-fmk
Viral titer ($TCID_{50}$ units/ml/24 h)	6.5 ± 0.3	5.6 ± 0.2*
Detached cell number (×10^4)	10.3 ± 0.8	5.5 ± 0.5*
LDH (units/l)	188 ± 10	194 ± 6

The results are expressed as the mean ± SEM from three different tracheae. Human tracheal epithelial cells were treated with a caspse-3 inhibitor Z-DEVD-fmk (1 μM) or vehicle (0.5% DMSO, dimethyl sulfoxide). Significant differences from the viral infection alone (A/H1N1 pdm 2009 + vehicle) are indicated by * $p < 0.05$.

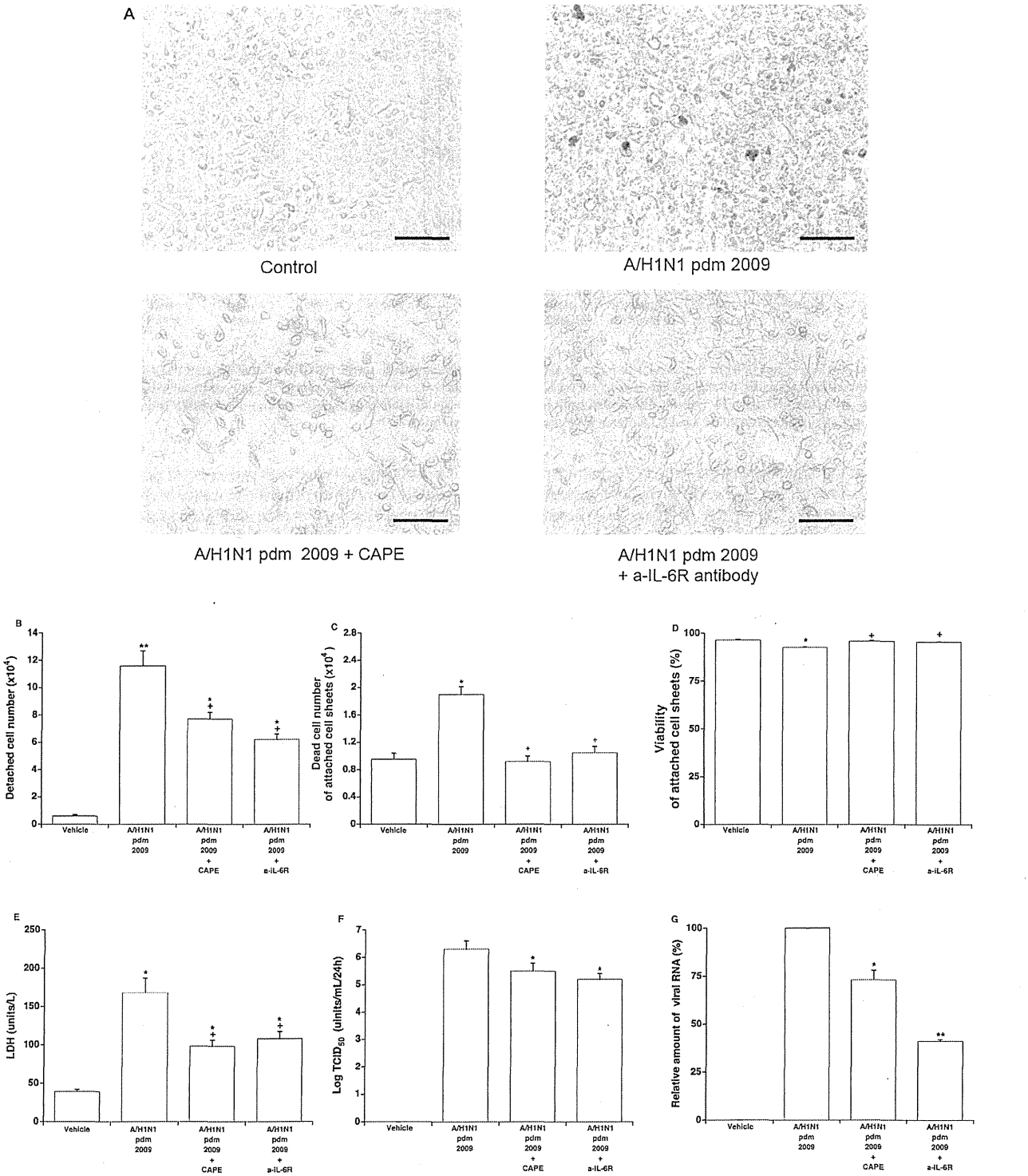

Fig. 3. (A) Phase contrast photographs of the primary cultures of human tracheal epithelial cells 5 days after infection with the A/H1N1 pdm 2009 virus and the vehicle (Control) in the presence of CAPE (A/H1N1 pdm 2009 + CAPE), a monoclonal anti-IL-6 receptor antibody (A/H1N1 pdm 2009 + a-IL-6R antibody) or vehicle (A/H1N1 pdm 2009). The surfaces of the confluent adhered cell sheets were covered with many detached floating cells from the sheets that were infected with the pandemic influenza virus (A/H1N1 pdm 2009). Treatment with CAPE and a monoclonal anti-IL-6 receptor antibody reduced the number of floating cells. Bar = 25 μm. (B)–(E): The number of detached cells (B), the number of dead cells and viability of adhered cell sheets ((C) and (D)), and the concentration of LDH (E) in the supernatants 5 days after exposure to the A/H1N1 pdm 2009 virus in the presence of CAPE (1 μM, A/H1N1 pdm 2009 + CAPE), an anti-IL-6 receptor antibody (1 μg/ml, A/H1N1 pdm 2009 + a-IL-6R) or the vehicle (A/H1N1 pdm 2009) or after the sham infection (Vehicle). The results are expressed as the mean ± SEM from four different tracheae. Significant differences from the sham infection are indicated by * $p < 0.05$ and ** $p < 0.01$. Significant differences from the viral infection alone are indicated by $^{+}$ $p < 0.05$. (F) and (G): Viral titers (F) in the supernatants and viral RNA (G) in the cells 5 days after exposure to the A/H1N1 pdm 2009 virus in the presence of CAPE (1 μM, A/H1N1 pdm 2009 + CAPE) or anti-IL-6 receptor antibody (1 μg/ml, A/H1N1 pdm 2009 + a-IL-6R) or exposure to the vehicle. Changes in the viral titers in the supernatants are expressed as $TCID_{50}$ units/ml/24 h. Viral RNA is expressed as the relative amount of RNA expression (%) compared with that of maximum viral RNA at day 5 in cells treated with the vehicle (A/H1N1 pdm 2009). The expression of viral RNA was normalized to the constitutive expression of β-actin mRNA. The results are expressed as the mean ± SEM from four different tracheae. Significant differences from the viral infection alone are indicated by * $p < 0.05$ and ** $p < 0.01$.

production may have enhanced influenza viral replication through NF-κB activation in the present study.

Infection with all of the four species of influenza virus activated both the NF-κB p50 and p65 subunits. Furthermore, the magnitude of p65 activation was associated with the magnitude of viral release, IL-6 production and the cell damage; however precise reasons are still uncertain regarding why only the p65 activation was associated with the magnitude of these factors. NF-κB increases the expression of genes for various pro-inflammatory cytokines (Zhu et al., 1996), and the production of interleukins is also associated with NF-κB p65 activation (Antal et al., 1996; More et al., 2013).

Influenza viral infection induces apoptosis through intrinsic and extrinsic pathways (Gao et al., 2013). The intrinsic pathway is mediated by members of the B-cell CLL/lymphoma 2 (Bcl-2) family and an apoptotic gene (Takizawa et al., 1993), and the extrinsic pathway is triggered by TNF family members (Gao et al., 2013). IL-6 is also associated with cell death and the activation of caspases in swine macrophages after pandemic A/H1N1 viral infection (Gao et al., 2012). In contrast, the induction of apoptosis of leukemia cells by suppressing NF-κB p65 has been reported (Ortiz-Lazareno et al., 2014). Partial inhibitory effects of the caspase-3 inhibitor on the cell detachment after virus infection, which were observed in the present study, may suggest the roles of caspase-3 activation induced by NF-κB-mediated-IL-6 production in the influenza viral infection-induced cell damage. However, we did not examine the effects of influenza virus infection on the activation of Bcl-2 family and apoptotic genes (Gao et al., 2013; Takizawa et al., 1993) in the present study. Further studies remain to clarify the mechanisms of cell damage after influenza virus infection.

The reason why the magnitude of virus replication was different among the four strains of virus is uncertain. However, virus stocks of the A/H1N1 pdm 2009 virus and the A/H1N1 Sendai virus were generated by infecting human tracheal epithelial cells with nasal swabs. In contrast, we generated virus stocks of the A/H3N2 New York virus and the A/H3N2 Aichi virus by infecting human tracheal epithelial cells with the viruses that had been passaged in MDCK cells. The serial passage of viruses in MDCK cells has been reported to reduce the potency of viral replication (Seladi-Schulman et al., 2013). The passage of viruses may influence the capability of virus replication.

In the present study, the titers of the four strains of type A influenza virus were detected for a prolonged duration of 7 days, which exceeds the duration reported by Boivin et al. (2000), who reported that significant viral titers in throat swabs were not detected 5 days (120 h) after the initiation of treatment with placebo. Although the reasons remain unclear, the absence of interferon in the supernatants, as demonstrated in the present study, might be partly associated with the long period of viral release from the cells in this study.

The dead cell number of attached cell sheets and the detached cell number and the LDH levels in the supernatants markedly increased after infection with A/H1N1 pdm 2009 virus in the present study. However, the viability measured by trypan blue exclusion was little affected. These results are consistent with those of Stark et al. (1991), who reported that LDH release is a more sensitive indicator of cell damage than trypan blue exclusion in human tracheal epithelial cells infected with parainfluenza viruses. These findings suggest that different assays may have different sensitivities for the detection of cell viability and cell damage after viral infection.

5. Conclusions

The magnitude of the detached cell number and the LDH levels in the supernatants of human tracheal epithelial cells was related to the magnitude of the replication of influenza viruses, the IL-6 production and the NF-κB p65 activation. Influenza viral infection-induced airway cell damage may be related to viral replication and subsequent NF-κB-p65-mediated IL-6 production.

Acknowledgements

This study was supported by Grant-in-Aid for Exploratory Research from Japan Society for the Promotion of Science (JSPS) KAKENHI Grant number 24659398.

References

Antal, J.M., Divis, L.T., Erzurum, S.C., Wiedemann, H.P., Thomassen, M.J., 1996. Surfactant suppresses NF-kappa B activation in human monocytic cells. Am. J. Respir. Cell Mol. Biol. 14, 374–379.

Boivin, G., Goyette, N., Hardy, I., Aoki, F., Wagner, A., Trottier, S., 2000. Rapid antiviral effect of inhaled zanamivir in the treatment of naturally occurring influenza in otherwise healthy adults. J. Infect. Dis. 181, 1471–1474.

Cai, Q., Lu, Z., Hong, G., Jiang, X., Wu, Z., Zheng, J., Song, Q., Chang, Z., 2012. Recombinant adenovirus Ad-RUNrf2 reduces paraquat-induced A549 injury. Hum. Exp. Toxicol. 31, 1102–1112.

Catalani, S., Carbonaro, V., Palma, F., Arshakyan, M., Galati, R., Nuvoli, B., Battistelli, S., Canestrari, F., Benedetti, S., 2013. Metabolism modifications and apoptosis induction after CellfoodTM administration to leukemia cell lines. J. Exp. Clin. Cancer Res. 32, 63.

Cechetti, F., Rhod, A., Simao, F., Santin, K., Salbego, C., Netto, C.A., Siqueira, I.R., 2007. Effect of treadmill exercise on cell damage in rat hippocampal slices submitted to oxygen and glucose deprivation. Brain Res. 1157, 121–125.

Cheung, C.Y., Poon, L.L.M., Lau, A.S., Luk, W., Lau, Y.L., Shortridge, K.F., Gordon, S., Guan, Y., Peiris, J.S.M., 2002. Induction of proinflammatory cytokines in human macrophages by influenza A (H5N1) viruses: a mechanism for the usual severity of human disease. Lancet 360, 1831–1837.

Condit, R.C., 2006. Principles of Virology. In: Knipe, D.M., Howley, P.M. (Eds.), Fields Virol, fifth ed. Lippincott Williams & Wilkins Inc., Philadelphia, PA, pp. 25–57.

Coulter, K.R., Doseff, A., Sweeney, P., Wang, Y., Marsh, C.B., Wewers, M.D., Knoell, D.L., 2002. Opposing effect by cytokines on Fas-mediated apoptosis in A549 lung epithelial cells. Am. J. Respir. Cell Mol. Biol. 26, 58–66.

de Jong, M.D., Simmons, C.P., Thanh, T.T., Hien, V.M., Smith, G.J., Chau, T.N., Hoang, D.M., Chau, N.V., Khanh, T.H., Dong, V.C., Qui, P.T., Cam, B.V., Ha, do Q., Guan, Y., Peiris, J.S., Chinh, N.T., Hien, T.T., Farrar, J., 2006. Fatal outcome of human influenza A (H5N1) is associated with high viral load and hypercytokinemia. Nat. Med. 12, 1203–1207.

Gao, R., Bhatnagar, J., Blau, D.M., Greer, P., Rollin, D.C., Denison, A.M., Deleon-Carnes, M., Shieh, W.J., Sambhara, S., Tumpey, T.M., Patel, M., Liu, L., Paddock, C., Drew, C., Shu, Y., Katz, J.M., Zaki, S.R., 2013. Cytokine and chemokine profiles in lung tissues from fatal cases of 2009 pandemic influenza A (H1N1): role of the host immune response in pathogenesis. Am. J. Pathol. 183, 1258–1268.

Gao, W., Sun, W., Qu, B., Cardona, C.J., Powell, K., Wegner, M., Shi, Y., Xing, Z., 2012. Distinct regulation of host responses by ERK and JNK MAP kinases in swine macrophages infected with pandemic (H1N1) 2009 influenza virus. PLoS One 7, e30328.

Garcia-Sastre, A., Egorov, A., Matassov, D., Brandt, S., Levy, D.E., Durbin, J.E., Palese, P., Muster, T., 1998. Influenza A virus lacking the NS1 gene replicates in interferon-deficient systems. Virology 252, 324–330.

Gyanchandani, R., Sano, D., Ortega Alves, M.V., Klein, J.D., Knapick, B.A., Oh, S., Myers, J.N., Kim, S., 2013. Interleukin-8 as a modulator of response to bevacizumab in preclinical models of head and neck squamous cell carcinoma. Oral Oncol. 49, 761–770.

Hsu, C.P., Chen, Y.L., Huang, C.C., Chou, C.C., Liu, C.L., Hung, C.H., Kao, T.Y., Chung, Y.C., 2011. Anti-interleukin-6 receptor antibody inhibits the progression in human colon carcinoma cells. Eur. J. Clin. Invest. 41, 277–284.

Kim, H.J., Kim, C.H., Ryu, J.H., Kim, M.J., Park, C.Y., Lee, J.M., Holtzman, M.J., Yoon, J.H., 2013. Reactive oxygen species induce antiviral innate immune response through IFN-regulation in human nasal epithelial cells. Am. J. Respir. Cell Mol. Biol. 49, 855–865.

Lipatov, A.S., Andreansky, S., Webby, R.J., Hulse, D.J., Rehg, J.E., Krauss, S., Perez, D.R., Doherty, P.C., Webster, R.G., Sangster, M.Y., 2005. Pathogenesis of Hong Kong H5N1 influenza virus NS gene reassortants in mice: the role of cytokines and B- and T-cell responses. J. Gen. Virol. 86, 1121–1130.

Lorusso, A., Faaberg, K.S., Killian, M.L., Koster, L., Vincent, A.L., 2010. One-step real-time RT-PCR for pandemic influenza A virus (H1N1) 2009 matrix gene detection in swine samples. J. Virol. Methods 164, 83–87.

Lu, C., Ren, D., Wang, X., Ha, T., Liu, L., Lee, E.J., Hu, J., Kalbfleisch, J., Gao, X., Kao, R., Williams, D., Li, C., 2014. Toll-like receptor 3 plays a role in myocardial infarction and ischemia/reperfusion injury. Biochim. Biophys. Acta 1842, 22–31.

Mauad, T., Hajjar, L.A., Callegari, G.D., da Silva, L.F., Schout, D., Galas, F.R., Alves, V.A., Malheiros, D.M., Auler Jr., J.O., Ferreira, A.F., Borsato, M.R., Bezerra, S.M., Gutierrez, P.S., Caldini, E.T., Pasqualucci, C.A., Dolhnikoff, M., Saldiva, P.H., 2010. Lung pathology in fatal novel human influenza A (H1N1) infection. Am. J. Respir. Crit. Care Med. 181, 72–79.

Mazur, I., Wurzer, W.J., Ehrhardt, C., Pleschka, S., Puthavathana, P., Silberzahn, T., Wolff, T., Planz, O., Ludwig, S., 2007. Acetylsalicylic acid (ASA) blocks influenza virus propagation via its NF-κB-inhibiting activity. Cell. Microbiol. 9, 1683–1694.

More, S.V., Park, J.Y., Kim, B.W., Kumar, H., Lim, H.W., Kang, S.M., Koppula, S., Yoon, S.H., Choi, D.K., 2013. Anti-neuroinflammatory activity of a novel cannabinoid derivative by inhibiting the NF-kB signaling pathway in lipopolysaccharide-induced BV-2 microglial cells. J. Pharmacol. Sci. 121, 119–130.

Natajaran, K., Singh, S., Burke Jr., T.R., Grunberger, D., Aggarwal, B.B., 1996. Caffeic acid phenethyl ester is a potent and specific inhibitor of activation of nuclear transcription factor NF-kappa B. Proc. Nat. Acad. Sci. U.S.A. 93, 9090–9095.

Nicholson, D.W., Ali, A., Thornberry, N.A., Vaillancourt, J.P., Ding, C.K., Gallant, M., Gareau, Y., Griffin, P.R., Labelle, M., Lazebnik, Y.A., Munday, N.A., Raju, S.M., Smulson, M.E., Yamin, T.T., Yu, V.L., Miller, D.K., 1995. Identification and inhibition of the ICE/CED-3 protease necessary for mammalian apoptosis. Nature 376, 37–43.

Nicholson, K.G., Kent, J., Ireland, D.C., 1993. Respiratory viruses and exacerbation of asthma in adults. Brit. Med. J. 307, 982–986.

Numazaki, Y., Oshima, T., Ohmi, A., Tanaka, A., Oizumi, Y., Komatsu, S., Takagi, T., Karahashi, M., Ishida, N., 1987. A microplate method for isolation of viruses from infants and children with acute respiratory infections. Microbiol. Immunol. 31, 1085–1095.

Ortiz-Lazareno, P.C., Bravo-Cuellar, A., Lerma-Diaz, J.M., Jave-Suarez, L.F., Aguilar-Lemarroy, A., Dominguez-Rodriguez, J.R., Gonzalez-Ramella, O., De Celis, R., Gomez-Lomeli, P., Hernandez-Flores, G., 2014. Sensitization of U937 leukemia cells to doxorubicin by the MG132 proteasome inhibitor induces an increase in apoptosis by suppressing NF-kappa B and mitochondrial membrane potential loss. Cancer Cell Int. 14, 13.

Perez-Padilla, R., de la Rosa-Zamboni, D., Ponce, de Leon, S., Hernandez, M., Quinones-Falconi, F., Bautista, E., Ramirez-Venegas, A., Rojas-Serrano, J., Ormsby, C.E., Corrales, A., Higuera, A., Mondragon, E., Cordova-Villalobos, J.A., INER Working Group on Influenza, 2009. Pneumonia and respiratory failure from swine-origin influenza A (H1N1) in Mexico. N. Engl. J. Med. 361, 680–689.

Presanis, A.M., De Angelis, D., New York City Swine Flu Investigation Team, Hagy, A., Reed, C., Riley, S., Cooper, B.S., Finelli, L., Biedrzycki, P., Lipsitch, M., 2009. The severity of pandemic H1N1 influenza in the United States, from April to July 2009: a Bayesian analysis. PLoS Med. 6, e1000207.

Rohde, G., Wiethege, A., Borg, I., Kauth, M., Bauer, T.T., Gillissen, A., Bufe, A., Schultze-Werninghaus, G., 2003. Respiratory viruses in exacerbations of chronic obstructive pulmonary disease requiring hospitalization: a case-control study. Thorax 58, 37–42.

Ruwanpura, S.M., McLeod, L., Miller, A., Jones, J., Bozinovski, S., Vlahos, R., Ernst, M., Armes, J., Bardin, P.G., Anderson, G.P., Jenkins, B.J., 2011. Interleukin-6 promotes pulmonary emphysema associated with apoptosis in mice. Am. J. Respir. Cell Mol. Biol. 45, 720–730.

Seladi-Schulman, J., Steel, J., Lowen, A.C., 2013. Spherical influenza viruses have a fitness advantage in embryonated eggs, while filament-producing strains are selected in vivo. J. Virol. 87, 13343–13353.

Shelton, H., Smith, M., Hartgroves, L., Stilwell, P., Roberts, K., Johnson, B., Barclay, W., 2012. An influenza reassortant with polymerase of pH1N1 and NS gene of H3N2 influenza A virus is attenuated in vivo. J. Gen. Virol. 93, 998–1006.

Stark, J.M., Huang, Y.T., Carl, J., Davis, P.B., 1991. Infection of cultured human tracheal epithelial cells by human parainfluenza virus types 2 and 3. J. Virol. Methods 31, 31–45.

Suzuki, T., Yamaya, M., Sekizawa, K., Hosoda, M., Yamada, N., Ishizuka, S., Yoshino, A., Yasuda, H., Takahashi, H., Nishimura, H., Sasaki, H., 2002. Erythromycin inhibits rhinovirus infection in cultured human tracheal epithelial cells. Am. J. Respir. Crit. Care Med. 165, 1113–1118.

Takizawa, T., Matsukawa, S., Higuchi, Y., Nakamura, S., Nakanishi, Y., Fukuda, R., 1993. Induction of programmed cell death (apoptosis) by influenza virus infection in tissue culture cells. J. Gen. Virol. 74, 2347–2355.

Wang, S., Le, T.Q., Kurihara, N., Chida, J., Cisse, Y., Yano, M., Kido, H., 2010. Influenza virus-cytokine-protease cycle in the pathogenesis of vascular hyperpermeability in severe influenza. J. Infect. Dis. 202, 991–1001.

Wen, W., Zhu, F., Zhang, J., Keum, Y.S., Zykova, T., Yao, K., Peng, C., Zheng, D., Cho, Y.Y., Ma, W.Y., Bode, A.M., Dong, Z., 2010. MST1 promotes apoptosis through phosphorylation of histone H2AX. J Biol. Chem. 285, 39108–39116.

Wurzer, W.J., Planz, O., Ehrhardt, C., Giner, M., Silberzahn, T., Pleschka, S., Ludwig, S., 2003. Caspase 3 activation is essential for efficient influenza virus propagation. EMBO J. 22, 2717–2728.

Yamaya, M., Finkbeiner, W.E., Chun, S.Y., Widdicombe, J.H., 1992. Differentiated structure and function of cultures from human tracheal epithelium. Am. J. Physiol. 262, L713–L724.

Yamaya, M., Nishimura, H., Hatachi, Y., Yoshida, M., Fujiwara, H., Asada, M., Nakayama, K., Yasuda, H., Deng, X., Sasaki, T., Kubo, H., Nagatomi, R., 2011. Procaterol inhibits rhinovirus infection in primary cultures of human tracheal epithelial cells. Eur. J. Pharmacol. 650, 431–444.

Yamaya, M., Shinya, K., Hatachi, Y., Kubo, H., Asada, M., Yasuda, H., Nishimura, H., Nagatomi, R., 2010. Clarithromycin inhibits type A seasonal influenza virus infection in human airway epithelial cells. J. Pharmacol. Exp. Ther. 333, 81–90.

Yan, H., Zhang, X., Luo, S., Liu, H., Wang, X., Gao, Y., Wilson, J.X., Huang, G., 2013. Effects of homocysteine on ERK signaling and cell proliferation in fetal neural stem cells in vitro. Cell. Biochem. Biophys. 66, 131–137.

Zhu, Z., Tang, W., Ray, A., Wu, Y., Einarsson, O., Landry, M.L., Gwaltney Jr., J., Elias, J.A., 1996. Rhinovirus stimulation of interleukin-6 in vivo and in vitro, Evidence for nuclear factor κB-dependent transcriptional activation. J. Clin. Invest. 97, 421–430.

OPEN ACCESS Freely available online

PLOS | ONE

Establishment and Clinical Applications of a Portable System for Capturing Influenza Viruses Released through Coughing

Etsuko Hatagishi[1,2], Michiko Okamoto[1], Suguru Ohmiya[1], Hisakazu Yano[1], Toru Hori[1], Wakana Saito[3], Hiroshi Miki[3], Yasushi Suzuki[4], Reiko Saito[4], Taro Yamamoto[2,5], Makoto Shoji[6], Yoshihisa Morisaki[7], Soichiro Sakata[8], Hidekazu Nishimura[1]*

1 Virus Research Center, Clinical Research Division, Sendai Medical Center, Sendai, Japan, **2** Department of International Health, Nagasaki University Graduate School of Biomedical Sciences, Nagasaki, Japan, **3** Department of Respiratory Medicine, Sendai Medical Center, Sendai, Japan, **4** Division of Public Health, Department of Infectious Disease Control and International Medicine, Graduate School of Medical and Dental Sciences, Niigata University, Niigata, Japan, **5** Department of International Health, Institute of Tropical Medicine, Nagasaki University, Nagasaki, Japan, **6** Shoji Clinic, Sendai, Japan, **7** Japan Self-Defense Force Sendai Hospital, Sendai, Japan, **8** Takasago Thermal Engineering Co., Ltd., Tokyo, Japan

Abstract

Coughing plays an important role in influenza transmission; however, there is insufficient information regarding the viral load in cough because of the lack of convenient and reliable collection methods. We developed a portable airborne particle-collection system to measure the viral load; it is equipped with an air sampler to draw air and pass it through a gelatin membrane filter connected to a cone-shaped, megaphone-like device to guide the cough airflow to the membrane. The membrane was dissolved in a medium, and the viral load was measured using quantitative real-time reverse transcriptase-polymerase chain reaction and a plaque assay. The approximate viral recovery rate of this system was 10% in simulation experiments to collect and quantify the viral particles aerosolized by a nebulizer. Using this system, cough samples were collected from 56 influenza A patients. The total viral detection rate was 41% (23/56), and the viral loads varied significantly (from <10, less than the detection limit, to 2240 viral gene copies/cough). Viable viruses were detected from 3 samples with ≤18 plaque forming units per cough sample. The virus detection rates were similar among different groups of patients infected with different viral subtypes and during different influenza seasons. Among patients who did not receive antiviral treatment, viruses were detected in one of six cases in the vaccinated group and four of six cases in the unvaccinated group. We found cases with high viral titers in throat swabs or oral secretions but very low or undetectable in coughs and vice versa suggesting other possible anatomical sites where the viruses might be mixed into the cough. Our system is easy to operate, appropriate for bedside use, and is useful for comparing the viral load in cough samples from influenza patients under various conditions and settings. However, further large-scale studies are warranted to validate our results.

Citation: Hatagishi E, Okamoto M, Ohmiya S, Yano H, Hori T, et al. (2014) Establishment and Clinical Applications of a Portable System for Capturing Influenza Viruses Released through Coughing. PLoS ONE 9(8): e103560. doi:10.1371/journal.pone.0103560

Editor: Hui-Ling Yen, The University of Hong Kong, Hong Kong

Received December 23, 2013; **Accepted** July 4, 2014; **Published** August 1, 2014

Funding: This work was supported by the annual budget for clinical research of Sendai Medical Center. The funders had no role in study design, data collection and analysis, decision to publish, or preparation of the manuscript.

Competing Interests: The authors have declared that no competing interests exist. Notably, as pointed out by the Editor that one of our authors (SS) is affiliated with a company, Takasago Thermal Engineering Co., Ltd., Tokyo. They would like to inform that he has been working mainly for basic technology which does not relate to the patent or products development, and this does not alter their adherence to all the PLOS ONE policies on sharing data and materials.

* Email: hide-nishimura@mte.biglobe.ne.jp

Introduction

Coughing plays an important role in the rapid spread of influenza infections among humans. Influenza virus-borne bio-particles are discharged from an infected person through coughing and transmitted to uninfected person(s). However, whether influenza virus particles are directly transmitted to the target host as large droplets or through inhalation by the host as small airborne particles remains controversial.

For example, Brankston et al. and Tellier reviewed many clinical and epidemiological studies, as well as experimental transmission studies using animal models and volunteers, and drew strikingly different conclusions: Brankston et al. did not support the airborne route [1], whereas Tellier advocated that the importance of the airborne route in the natural transmission of influenza infections [2,3]. To address these controversies, Wong et al. [4] conducted a spatiotemporal analysis during an influenza outbreak in a hospital ward and reported that infections spread along the direction of airflow from the index case. Furthermore, Lindsley et al. [5] and Blachere et al. [6] detected the airborne virus in healthcare facilities treating influenza patients. Thus, it is important to assess airborne transmission to discern the amount of virus released into environmental air through coughing.

Recently, viral RNA was detected in voluntary cough samples of influenza patients by many researchers using their own methods. For example, Stelzer-Braid et al. [7] used a continuous positive airway pressure mask with a collection disk composed of a dielectric material, and Lindsley et al. [8] used a biosampler (SKC Inc., Eighty Four, PA, USA) and a two-stage bioaerosol cyclone

sampler (National Institute for Occupational Safety and Health, Pittsburgh, PA, USA). Moreover, Bischoff et al. [9] collected viruses by sampling room air for >20 min using the Andersen impaction air sampler (Thermo Fisher Scientific, Waltham, MA, USA) placed close to the patient, and Milton et al. [10] used self-produced G-II sampler designed for collection of the exhaled breath and cough. However, the systems used in the aforementioned studies did not appear to be optimal for collecting samples from many subjects in medical settings or common areas, because of issues of burden to patients, portability and simplicity.

In the present study, we developed a portable system to easily collect bio-particles released by coughing at bedside within a short time without burdening the patients (Figure 1), and quantified the viral load with a definite recovery rate. The methodology and collection results from influenza cases under various conditions, such as status of vaccination and antiviral treatment, as well as possible applications for analyses of the effects of these interventions are discussed. Furthermore, combining the viral load data of the cough samples with those of throat swabs and oral secretions, we propose some interesting possibilities regarding the anatomical sites where the viruses might be mixed with a cough.

Materials and Methods

Ethics Statement

This study was approved by the ethical committee of Sendai Medical Center (Sendai City, Miyagi Prefecture, Japan), and written informed consent was obtained from all patients.

Device for collection of bio-particles

Airborne particles in coughs and mists, generated in laboratory experiments to simulate coughs, were collected using an airborne particle-sampling unit composed of portable air sampler (MD8 AirScan Sartorius AG, Göttingen, Germany) connected by a flexible polyvinyl chloride hose with reinforced ends (#17085; inner diameter, 32 mm; length, 2 m; Sartorius AG) (Figure 1A) to a gelatin membrane filter (#12602-080-ALK; diameter, 8.0 cm; pore size, 3.0 μm; Sartorius AG) (Figure 1 A, C) and equipped with a cone-shaped, megaphone-like device (length, 50 cm; entrance diameter, 40 cm) made of a polycarbonate resin sheet (Figure 1 A, B) to guide the airflow to the membrane. The outer surface of the device was coated with aluminum foil to reduce the static electric charge of the inner surface.

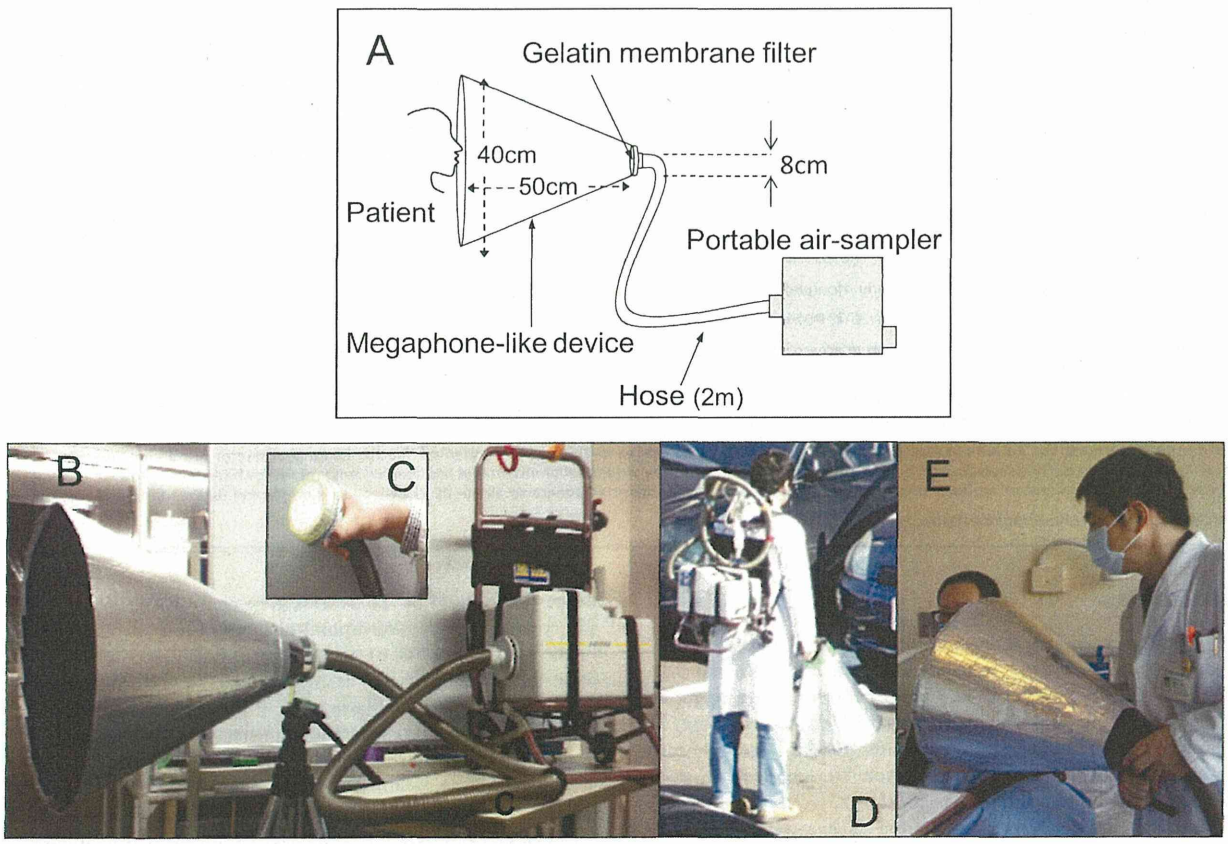

Figure 1. The system cough collection developed in this study. A schematic diagram of the total system (A). A picture of the composition: the pump, hose, and cone shaped, megaphone-like device, from the right (B). The gelatin membrane filter (C) was attached to end of the hose and connected to the tip of the cone to entrap the particles passing in the airflow. The complete system is portable, even on ones back (D), and can be easily used in many situations, especially at bedside (E).
doi:10.1371/journal.pone.0103560.g001

Collection of clinical samples

Cough, throat swab and oral samples were collected, in this order, from individuals exhibiting symptoms of influenza who visited one of three medical facilities in Sendai City, Japan. Among them, those who received final diagnosis of influenza by viral isolation from throat swab samples were enrolled in this study. Samples from 16 patients from Sendai Medical Center (average age, 32.4 ± 16.6 years), 39 from Japan Self-Defense Force Sendai Hospital (average age, 22.1 ± 3.2 years), and 1 from Shoji Clinic (age, 44 years) were collected from January 2008 to February 2011 and included for analysis.

For sample collection, patients were asked to cough voluntarily approximately 20 times at their own pace and without great effort into the cone entrance toward the gelatin membrane filter, which was at the opposing tip of the cone. The connected sampler was set at a constant airflow rate of 8.0 m^3/h, which is the maximum pumping rate according to the manufacturer and was previously adopted in a swine influenza study [11]. The pumping duration was from 1 min before the start of coughing and continued until at least 1 min after the last cough. The filter to trap the bio-particles was cooled immediately after collection until it was transported to the laboratory where it was then dissolved in 10 mL of Eagle's minimum essential medium (MEM; Sigma-Aldrich, St. Louis, MO, USA) supplemented with 50 U of penicillin and 50 μg/mL of streptomycin at 37°C. The samples were aliquoted and then assessed using a plaque assay, whereas the remaining samples were stored at −80°C until quantification of the viral gene copy number. Throat swabs were collected from the pharyngeal walls exclusively by one of the investigators (E.H.) to avoid technical variation in sampling techniques by multiple collectors using cotton swabs. Then, the swabs were vigorously washed in MEM transport medium supplemented with 50 U of penicillin and 50 μg/mL of streptomycin. The oral secretions consisted mainly of saliva and mucus produced by the oral membrane and/or mucus brought by a cough from the deeper respiratory tract was spat by patients in Petri dishes.

Virus and devices for airborne experiments

Influenza virus A/Aichi/2/68 (H3N2) was propagated in the allantoic cavities of fertilized chicken eggs. The allantoic fluid containing the viruses was harvested and atomized in simulation experiments using an electric compressor nebulizer (NE-C16; Omron, Kyoto, Japan).

Concentration and quantification of the viruses eluted in the gelatin solution

The gelatin membrane was dissolved in 10 mL of MEM and treated with 10 μg/mL of collagenase (Collagenase S-1, Nitta Gelatin, Osaka, Japan) at 37°C for 1 h and ultra-centrifuged at 125,000 g for 100 min to obtain viral precipitate, which was then dissolved in extraction buffer included with the RNA extraction kit (QIAamp Viral RNA Mini Kit, Qiagen, Valencia, CA, USA); the viral RNA was extracted in 80 μL of RNAse-free water according to the manufacturer's instructions. The RNA solution was concentrated using a freeze-drying system composed of a freeze dryer (FD-80; Eyela; Tokyo Rikakikai Co., Ltd., Tokyo, Japan), a centrifugal concentrator (VC-12S; TAITEC, Saitama, Japan), and a vacuum pump (MFG; Hitachi, Tokyo, Japan). The total amount of extracted RNA was used for complementary DNA (cDNA) synthesis using the reverse transcription kit (High-Capacity cDNA Reverse Transcription Kit, Applied Biosystems, Foster City, CA, USA) with random primers following the manufacturer's protocol. The amount of generated cDNA was measured with quantitative real-time reverse transcriptase-polymerase chain reaction (qRT-PCR) using the MiniOpticon system with CFX Manager software (Bio-Rad Laboratories, Hercules, CA, USA), influenza A matrix protein 1 (M1)-specific primers, and probes designed by Daum et al. [12]. All reactions were performed in 48-well plates in duplicate or triplicate. A standard curve was generated from 10-fold serial dilutions of the RNA from the M1 cDNA of influenza virus strain A/Aichi/2/68. Negative controls without templates were included in each plate.

Viral isolation and plaque assay

Throat swab samples in MEM transport medium were centrifuged at low-speed (1500 g) for 15 min, and then inoculated onto Madin-Darby canine kidney (MDCK) cells for viral culture [13]. Viral isolation was assessed within a week by identifying the specific cytopathic effect. The dissolved membrane specimens containing viruses of the coughs were the serially diluted 10-fold with MEM and inoculated onto MDCK cells. The diluted specimens were assessed for active viruses using a conventional plaque assay [14] within 1 h after collection.

Results

System establishment for viral collection and quantification

The collection system was equipped with a portable air sampler unit containing a gelatin membrane filter and a large cone-shaped, megaphone-like device to guide the expelled particles to the filter (Figure 1 A, B). The length and maximum diameter of the cone were 50 and 40 cm, respectively, which was based on information on cough airflow provided by *schlieren* (German word, indicating optical inhomogeneities) analysis, as per the report by Tang et al. [15] and our recent study of vector analysis [16]. These two reports estimated the range of the momentum of coughs to be approximately 30 cm or less from the participant's mouth and thereafter, the particles spread by diffusion. Considering this assumption, the length of the device was determined as 50 cm to include possible outlier cases. The particle velocity by coughing should slow down at the filter to at least less than that of the suctioning airflow (0.56 m/s, theoretically calculated).

To evaluate the efficiency of our system to measure the total viral load in a cough, we attempted to separately estimate the rough recovery rates of the collection and quantification processes.

For the collection process, experiments to simulate human coughing were performed using a nebulizer. Size distribution patterns of the particles were confirmed to be mostly resembled between the mist of the nebulizer and human coughs (Figure S1). First, the viral fluid containing approximately 10^8 plaque forming units (PFU)/mL of influenza virus was atomized by a nebulizer every 0.5 s for 3 s, which was repeated 10 times, and directed toward a gelatin membrane filter set 10 cm from the nebulizer. The generated viral mist was drawn directly into the gelatin filter membrane apparently by robust pumping of the sampler, which was confirmed against a black paper background and was visible by the naked eye. A similar experiment was repeated using a hollow paper tube (length, 10 cm; inner diameter, 8 cm) to guide the mist to the membrane, of which the outer and inner surfaces were coated with aluminum foil to prevent static charge (Figure 2 A). This tube was placed to minimize the possibility that the